Electronic Supplementary Material (ESI) for Journal of Materials Chemistry B.

Supporting Information

Thiophene-Based Organic Dye with Large Stokes Shift and Deep Red Emission for Live Cell NAD(P)H Detection under Varying Chemical Stimuli

Sushil K. Dwivedi,[a,b] Dilka Liyana Arachchige,[a,b] Adenike Olowolagba,[a,b] Mohamed Mahmoud,[a,b] Jenna Cunnien,[a,b] Daniel R. Tucker,[a] Delaney Fritz,[c] Thomas Werner,[c] Rudy L Luck[a]* and Haiying Liu[a]*

[a]Department of Chemistry, [b]Health Research Institute, [c]Department of Biological Sciences, Michigan Technological University, Houghton, MI 49931. E-mail: rluck@mtu.edu and hyliu@mtu.edu

Table of Contents

Synthesis of fluorescent probes

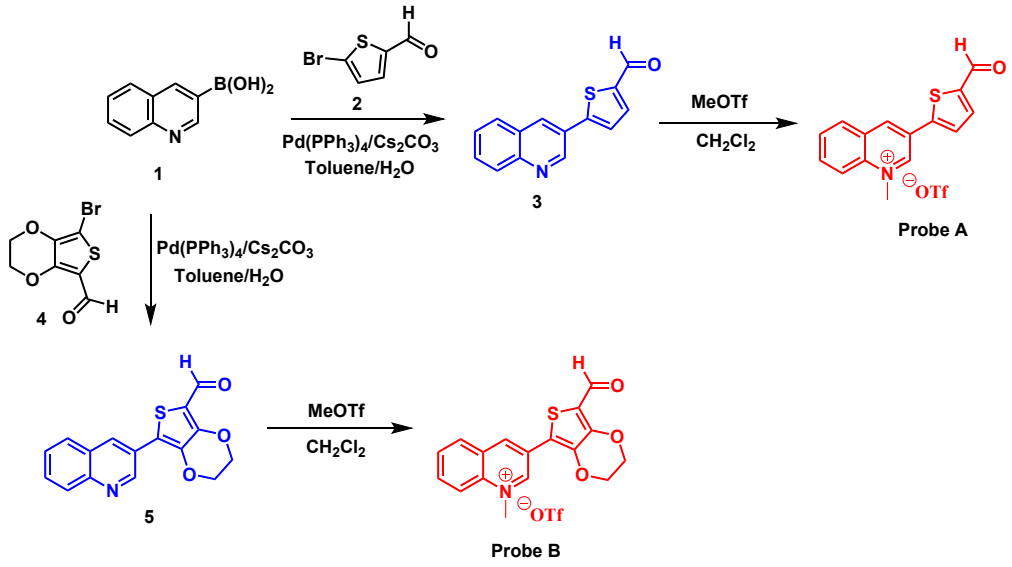

Scheme 1. Synthetic approach to prepare fluorescent probes.

Synthesis of compound 3: In a 50 mL round bottom flask, 500.0 mg (2.89 mmol) of quinolin-3-ylboronic acid and 552.20 mg (2.89 mmol) of 5-bromothiophene-2-carbaldehyde were combined with 20 mL of a toluene/H_2O mixture (9:1) under a nitrogen atmosphere. A small amount of palladium tetrakiss(triphenylphosphene) (5% by mol) and 2.5 equivalents of cesium carbonate were then added to the mixture, and the reaction was heated at 90°C for 8 hours. The reaction was confirmed complete by TLC, and the reaction mixture was cooled before the solvent was removed under reduced pressure. The residue was treated with ice-cold water and extracted using dichloromethane (3 extractions, 20 mL). The combined organic layer was dried with sodium bicarbonate and evaporated under reduced pressure to yield a light-yellow solid. Purification by column chromatography produced a compound **3** with a 60% yield.^{1}H NMR (400 MHz, DMSO-d_6), δ (ppm): 7.76 (1H, m), 7.82 (1H, m), 8.03 (1H, d, J = 12.0 Hz), 8.08 (2H, d, J = 8 Hz), 8.14 (1H, d, J = 4.0 Hz), 8.82 (1H, s), 9.37 (1H, s), 9.98 (1H, s).

Synthesis of Probe A: A solution of compound **3** (100.0 mg, 0.41 mmol) in 20 mL of dry dichloromethane was prepared and methyl trifluoromethanesulfonate (75.5 mg, 0.45 mmol) was added to the mixture. The reaction mixture was stirred at room temperature under a nitrogen

atmosphere for 6 hours, which led to the formation of a light-yellow precipitate, yielding Probe **B**. The precipitate was filtered and washed with cold dichloromethane (3 times, 5 mL each). ^{1}H NMR (400 MHz, DMSO-d_6), δ (ppm): 4.71 (3H, s), 8.09 (2H, m), 8.23 (1H, d, *J* = 4.0 Hz), 8.29 (1H, t, *J* = 6.0 Hz), 8.49 (2H, m), 9.68 (1H, s), 10.04 (1H, s), 10.09 (1H, s). ^{13}C NMR (101 MHz, DMSO-d_6,) δ (ppm): 46.04, 119.74, 127.26, 129.26, 129.56, 131.17, 131.27, 136.33, 138.07, 139.31, 142.58, 145.13, 145.21, 149.04, 185.13. LCMS (m/z): 254.17

Synthesis of compound 5: In a 50 mL round-bottomed flask, a mixture of quinolin-3-ylboronic acid (500.0 mg, 2.89 mmol) and 7-bromo-2,3-dihydrothieno[3,4-b][1,4]dioxine-5-carbaldehyde (719.84 mg, 2.89 mmol) was prepared using 20 mL of a 9:1 mixture of toluene and water. Under a nitrogen atmosphere, a small quantity of palladium tetrakiss(triphenylphosphene) (5 mol%) and cesium carbonate (2.5 equiv.) were added to the mixture, which was then heated at 90°C for 8 hours. Completion of the reaction was confirmed by TLC, following which the reaction mixture was cooled and the solvent was removed under reduced pressure. The residue was treated with ice-cold water and extracted three times with dichloromethane. The combined organic layer was dried over sodium bicarbonate and evaporated under reduced pressure, resulting in a crude light-yellow solid. Purification of the crude product by column chromatography yielded compound **5** as a yellow solid, with a yield of 65%. ^{1}H NMR (400 MHz, $CDCl_3$), δ (ppm): 4.49 (4H, s), 7.58 (1H, t, 8.0 Hz), 7.74 (1H, t, J = 6.0 Hz), 7.78 (2H, d, J= 8 Hz), 8.11 (1H, d, J= 8.0 Hz), 8.54 (1H, s), 9.32 (1H, s), 10.0 (1H, s).

Synthesis of Probe B: To dissolve compound **5** (100.0 mg, 0.33 mmol), 20 mL of dry dichloromethane was employed, and subsequently, 60.71 mg (0.36 mmol) of methyl trifluoromethanesulfonate was added to the mixture. The resulting mixture was stirred at room temperature for 6 hours under a nitrogen-filled atmosphere, leading to the formation of a yellow precipitate. The precipitate was then filtered and washed with cold dichloromethane for 5 cycles, yielding Probe **B**.^{1}H NMR (400 MHz, DMSO-d_6), δ (ppm): 4.60 (4H, s), 4.72 (3H, s), 8.07 (1H, m), 8.29 (1H, m), 8.51 (1H, m), 8.55 (2H, d, J= 4.0 Hz), 9.55 (1H, s), 9.81 (1H, s), 10.01 (1H, s). ^{13}C NMR (101 MHz, DMSO-d_6,) δ (ppm): 46.26, 65.82, 65.96, 117.92, 118374, 119.74, 126.20, 129.55, 131.12, 131.19, 136.21, 137.79, 141.56, 142.39, 148.49, 149.33, 180.67. LCMS (m/z): 312.11.

Instrumentation

The ^{1}H (500 MHz) and ^{13}C (125 MHz) NMR spectra were acquired using a Bruker NMR spectrometer (Ascend 500) in DMSO-d_6 and $CDCl_3$ (2.0×10^{-2} M). The absorption and emission spectra of the probe were measured using a PerkinElmer Lambda 35 UV/vis spectrometer and a Jobin Yvon Fluoromax-4 spectrofluorometer, respectively. The mass spectra of the probe and its reduced product were recorded using a Thermo scientific LCQ Fleet mass spectrometry. Confocal images were captured using an OLYMPUS FLUOVIEW FV1000. Stock solutions of probe **A**, probe **B**, NADH, NADPH, and other analytes were prepared in pH 7.4 phosphate-buffered saline.

Reagents

The experiment utilized a variety of reagents including metal ions, cysteine, glutathione, carbohydrates, amino acids, and other chemicals. These reagents were purchased from commercial vendors and used in their original form. Additionally, cyanine dye (IR-780) was also utilized in the experiment.

Cell culture

All experiments were performed by exposing A549 cells to 5 μM of either probe **A** or **B** for 1 hour. In the NADH-dependent study, the A549 cells were first incubated with various concentrations of NADH (20, 50, 100 μM) in DMEM medium for 1 hour, followed by treatment with 5 μM of probe **A** or **B** for an additional hour. In the glucose-dependent study, A549 cells were pre-treated with 0, 5, 10, and 20 mM of glucose in serum-free DMEM medium for 1 hour before exposure to 5 μM of probe **A** or **B** for 1 hour. The pyruvate/lactate-dependent studies involved pre-treating A549 cells with 10 mM lactate, 5 mM pyruvate, or a combination of 10 mM lactate and 5 mM pyruvate for 1 hour in serum-free DMEM medium before exposure to 5 μM of probe **A** or **B** in serum-free DMEM medium for 1 hour.

For investigating the influence of FCCP, the A549 cells were initially exposed to 5 μM FCCP for 15 minutes in serum-free DMEM medium, followed by treatment with either probe **A** or **B** for 1 hour.

Colocalization Study

To perform the colocalization analysis, A549 cells were initially treated with 50 mM glucose in serum-free DMEM medium for 30 minutes. Following this, the cells were exposed to a mixture of 5 μM of probe **A** or **B** and a cyanine dye (IR-780) in serum-free DMEM medium for 60 minutes.

Hypoxia experiment

In order to study the NADH levels under hypoxic conditions, we subjected A549 cells to pre-treatment with different concentrations of $CoCl_2$ (50, 100, and 150 μM) for a duration of 12 hours. Subsequently, the cells were incubated with either 5 μM of probe **A** or **B** in serum-free and glucose-free DMEM medium for a period of 60 minutes to assess their impact.

Drug treatment of A459 cells

The impact of cisplatin on NAD(P)H levels in A549 cells was investigated by treating the cells with 20 μM cisplatin in DMEM medium without serum and glucose for 6 and 24 hours. Subsequently, the cells were incubated with either 5 μM probe A or B in serum-free and glucose-free DMEM medium for 60 minutes to determine its effect.

To investigate how gemcitabine affects NAD(P)H levels in A549 cells, the cells were treated with different concentrations of gemcitabine (5 μM, 10 μM, and 20 μM) in DMEM medium without serum for two hours. Subsequently, we incubated the cells with either 5 μM of probe A or 5 μM of a previously reported fluorescent probe (ACS Sensor 2016, 1(6), 702-709) in serum-free and glucose-free DMEM medium for 30 minutes to analyze the impact. We chose the same 30-minute incubation time for both probes to ensure fair comparison.

***D. melanogaster* larval imaging**

The wild-type *D. melanogaster* fly stock Canton-S was utilized. Female flies were given the opportunity to deposit their eggs on agar plates supplemented with sucrose and Baker's yeast. After an 8-hour incubation period, the eggs were collected, and the yeast was removed to prepare for the hatching of the larvae. Once hatched, the larvae were gathered using a pin and thoroughly rinsed twice with 1 mL of PBS. The larvae were then subjected to a 6-hour incubation

with 5 μM probe **A** or **B** in pH 7.4 phosphate buffer solutions. To complete the process, the larvae were washed three times for 10 minutes each with PBS and placed on a glass slide beneath a coverslip for fluorescence imaging under 488 nm excitation.

D. melanogaster flies were allowed to lay eggs on sugar agar plates with Baker's yeast and were kept at room temperature with a 12:12-h light/dark cycle. The eggs were collected in the early morning and late afternoon using a moist brush and were subsequently washed and placed on Petri dishes on top of damp paper towels. After two days of incubation at 18°C, the larvae hatched and were transferred to glass viewing dishes for staining experiments. Any larvae that died of starvation during the experiment were removed during washes. The larvae hatched from starvation were incubated in different NADH concentrations, ranging from 0 to 100 μM in aqueous solutions, and then washed three times with aqueous solutions before being further incubated with 5 μM probe **A** in PBS solution for one hour. After being washed three times with PBS for 10 minutes each time, the larvae were mounted on a glass slide with a coverslip for fluorescence imaging using 488 nm excitation.

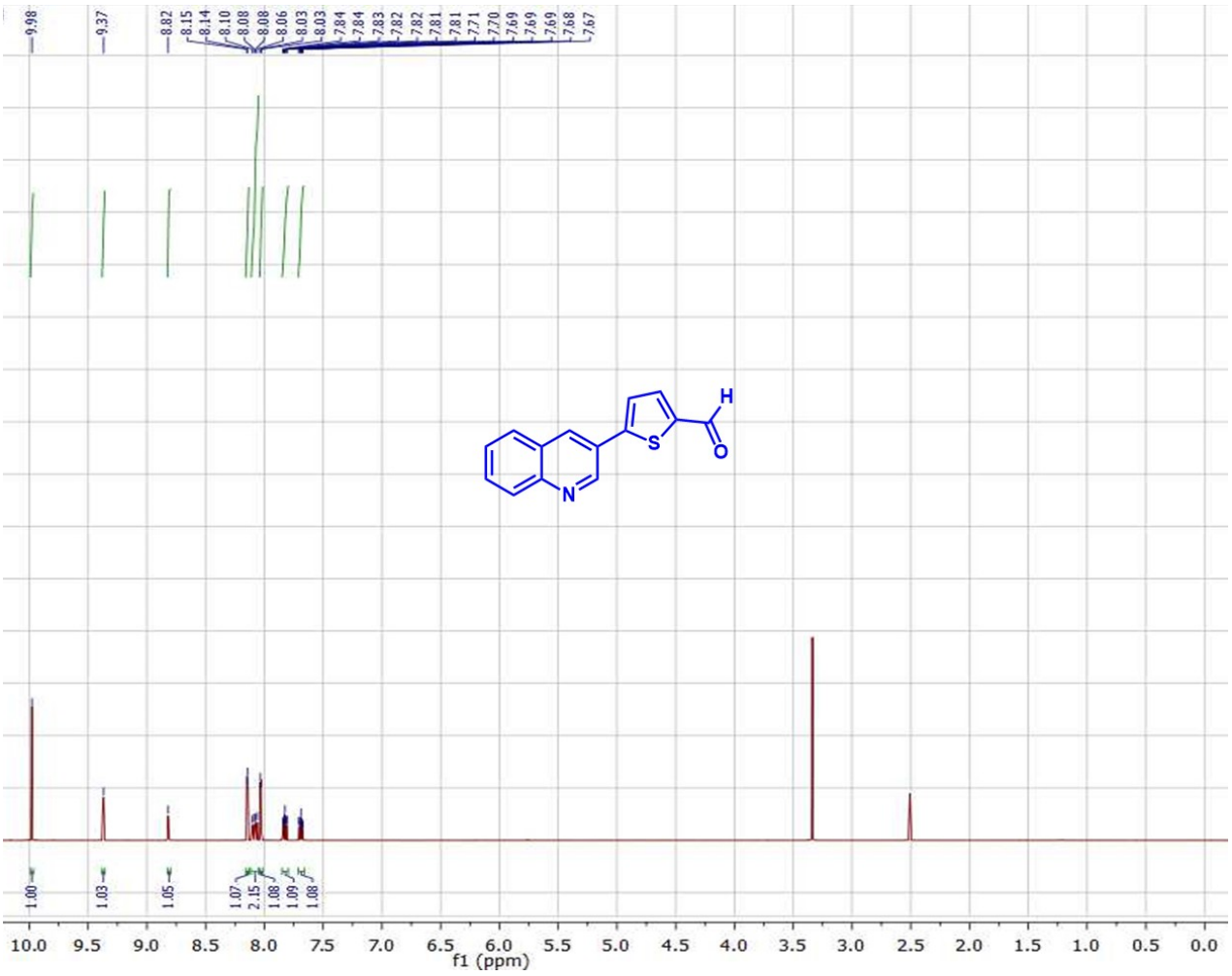

Figure S1: ^{1}H NMR spectrum of compound **3** in DMSO-d_6 solution.

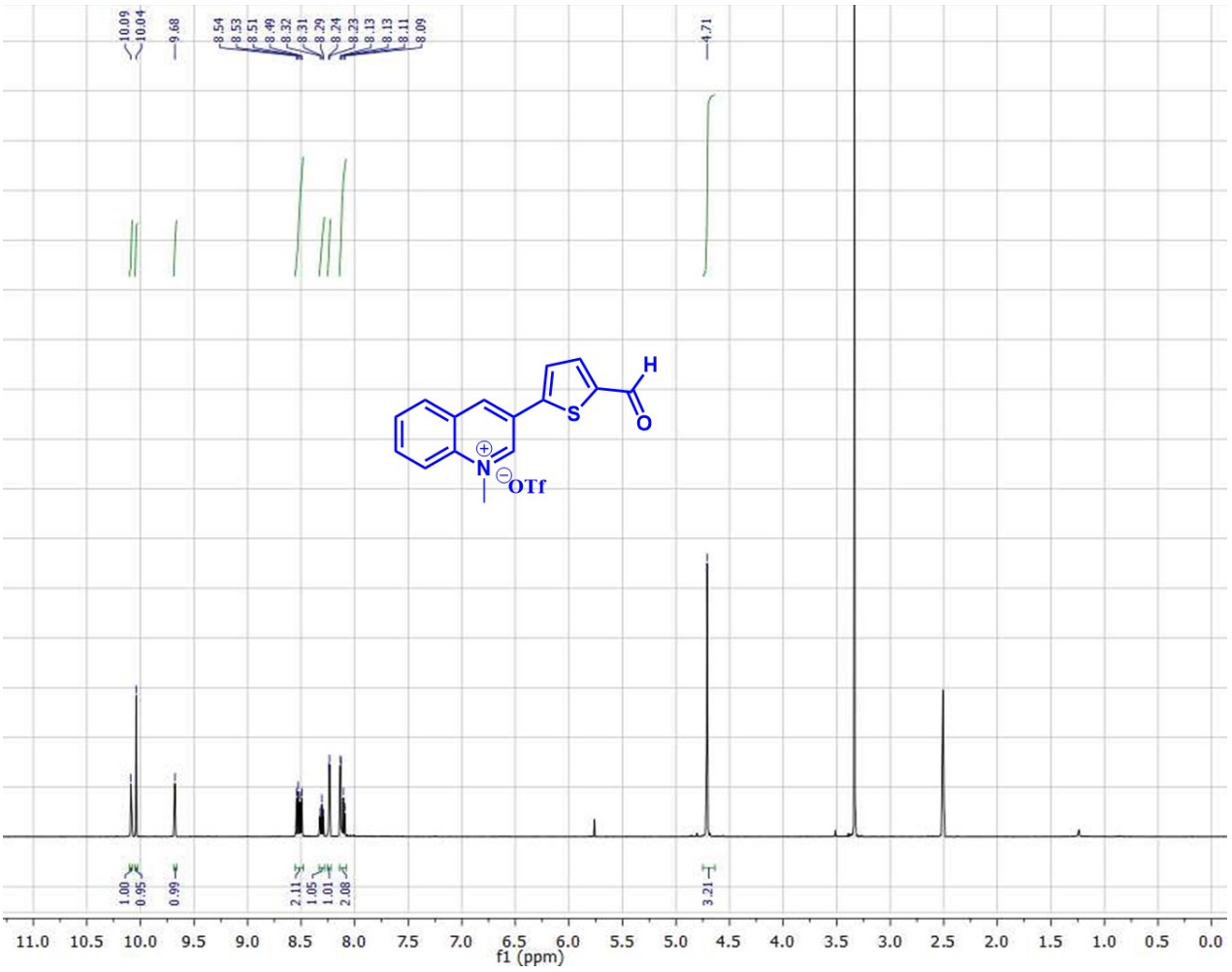

Figure S2: ^{1}H NMR spectrum of Probe **A** in DMSO-d_6 solution.

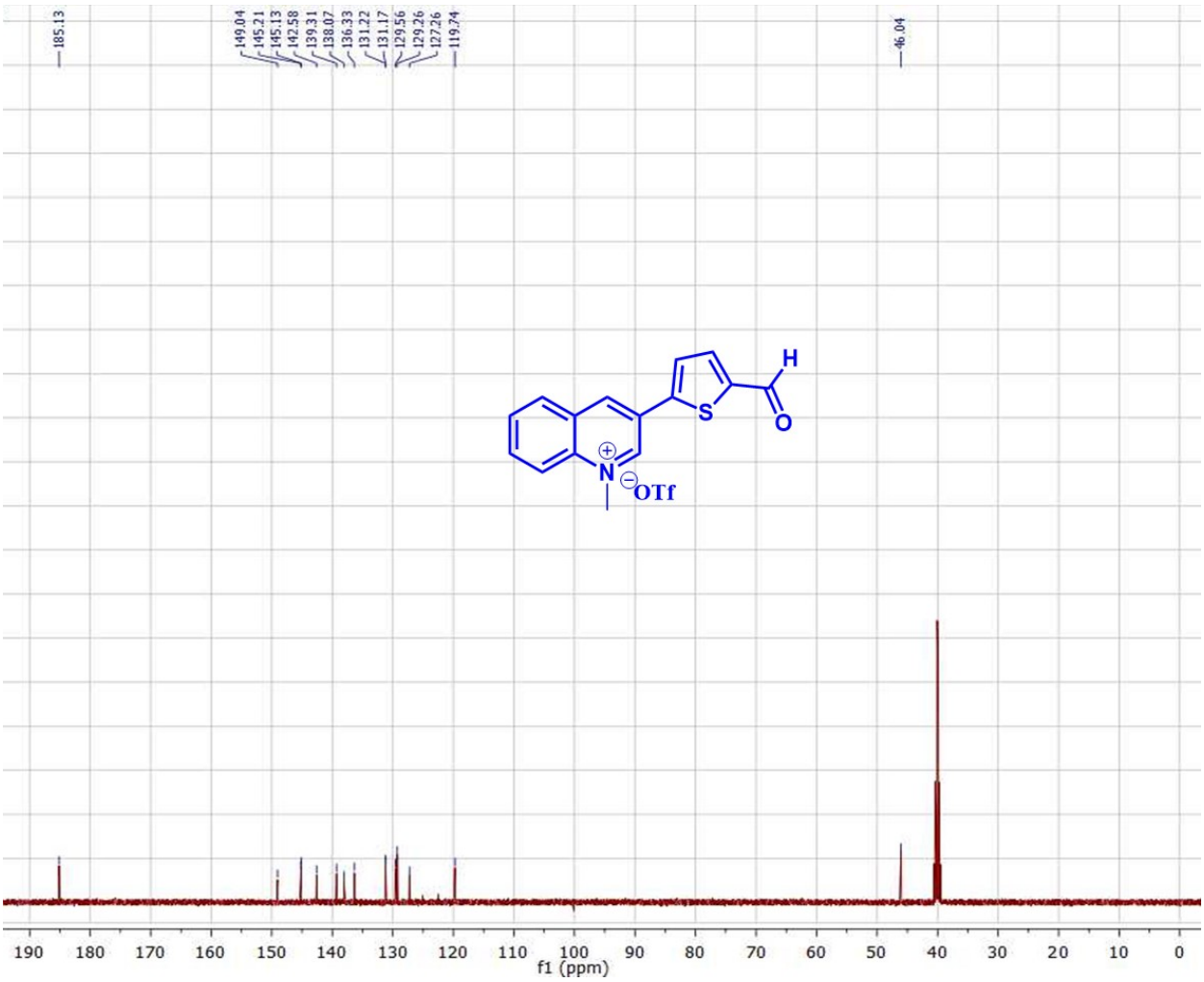

Figure S3: ^{13}C NMR spectrum of Probe **A** in DMSO-d_6 solution.

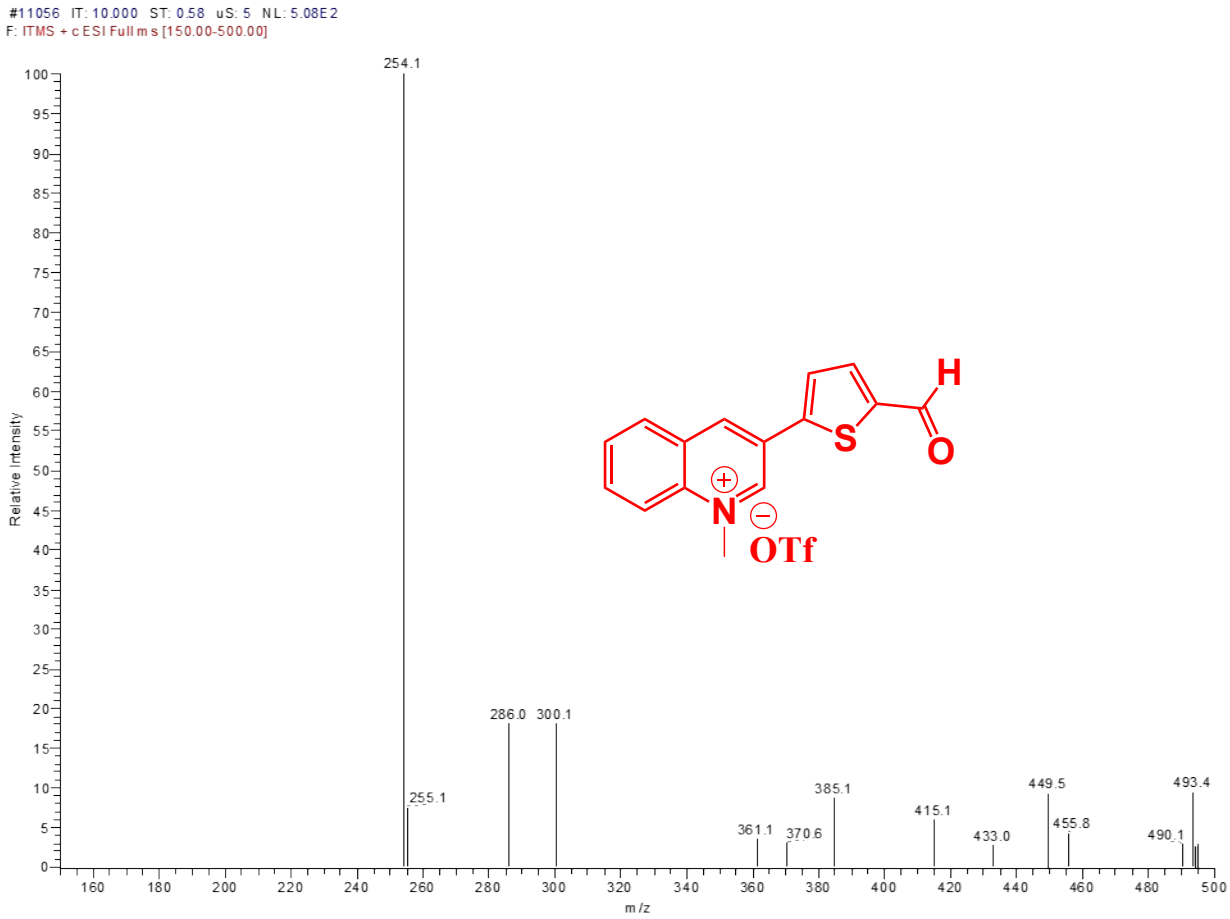

Figure S4: Electrospray MS spectrum of Probe **A**.

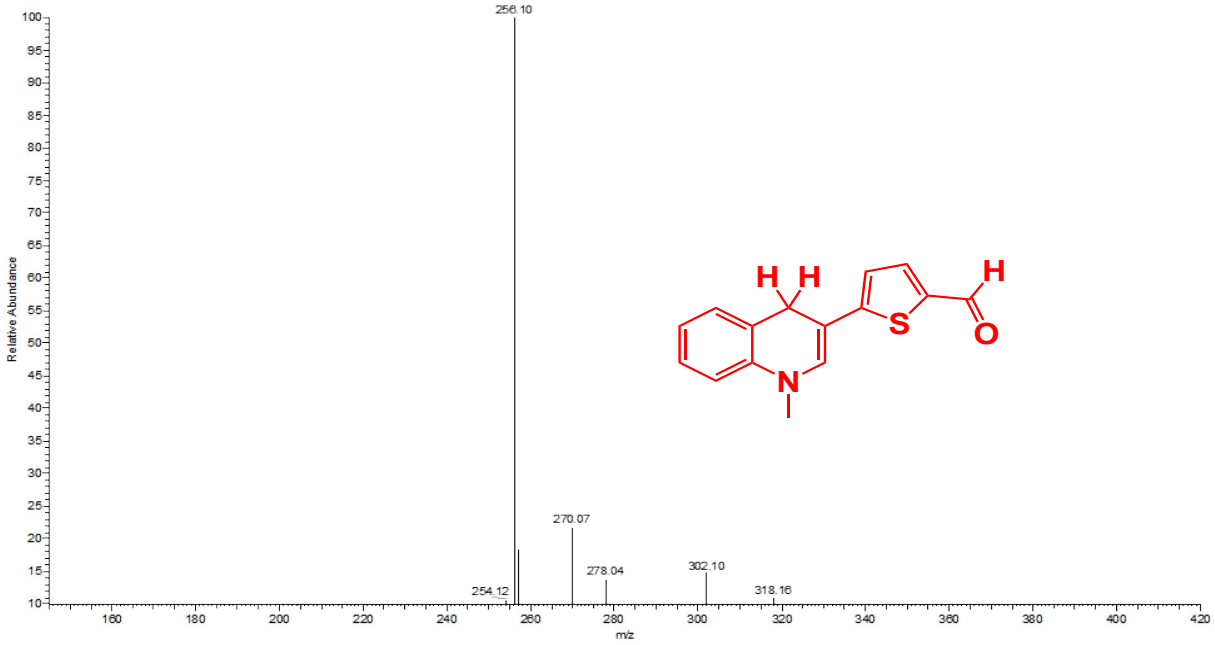

Figure S5: Electrospray MS spectrum of Probe **AH**.

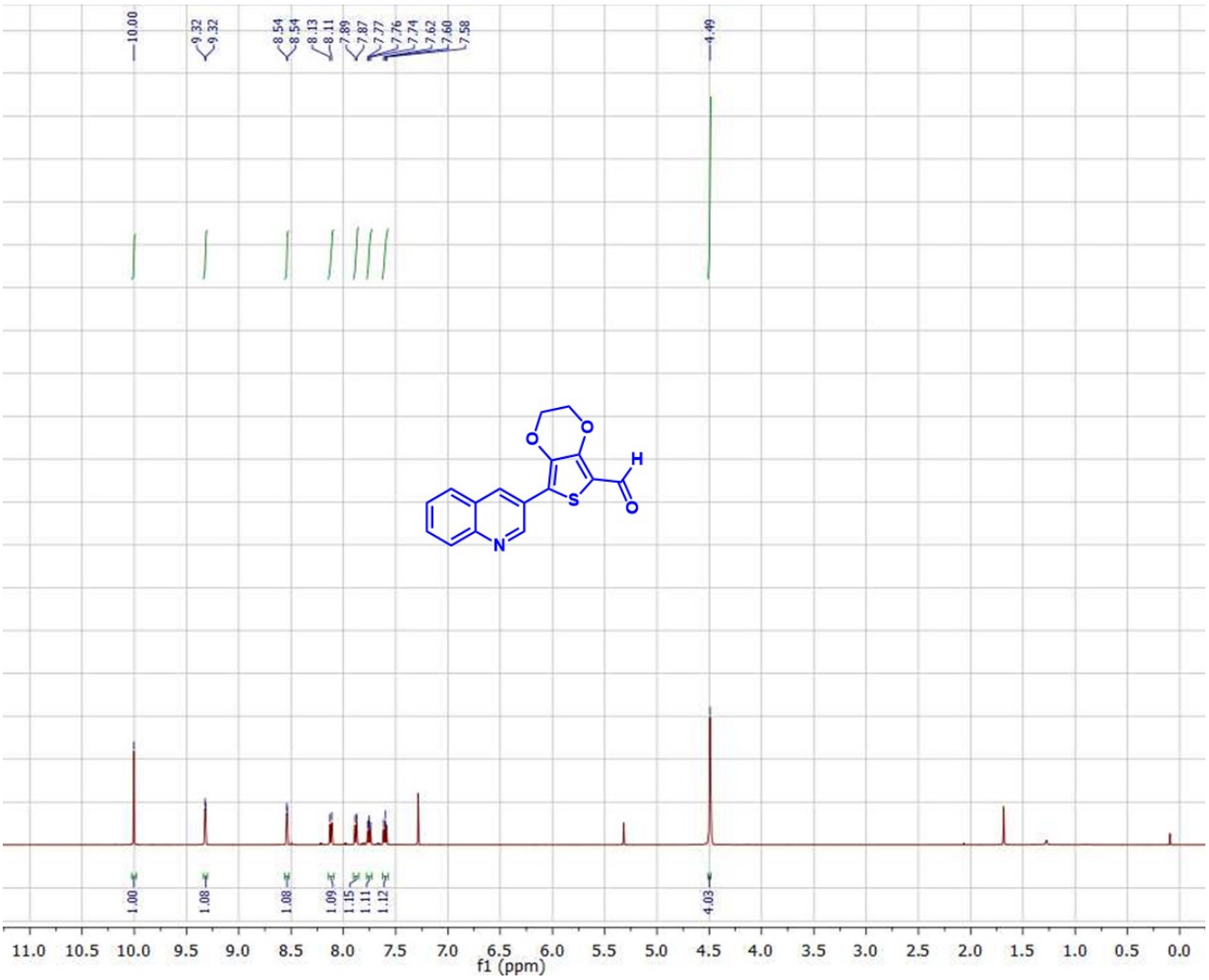

Figure S6: ^{1}H NMR spectrum of compound **5** in $CDCl_3$ solution.

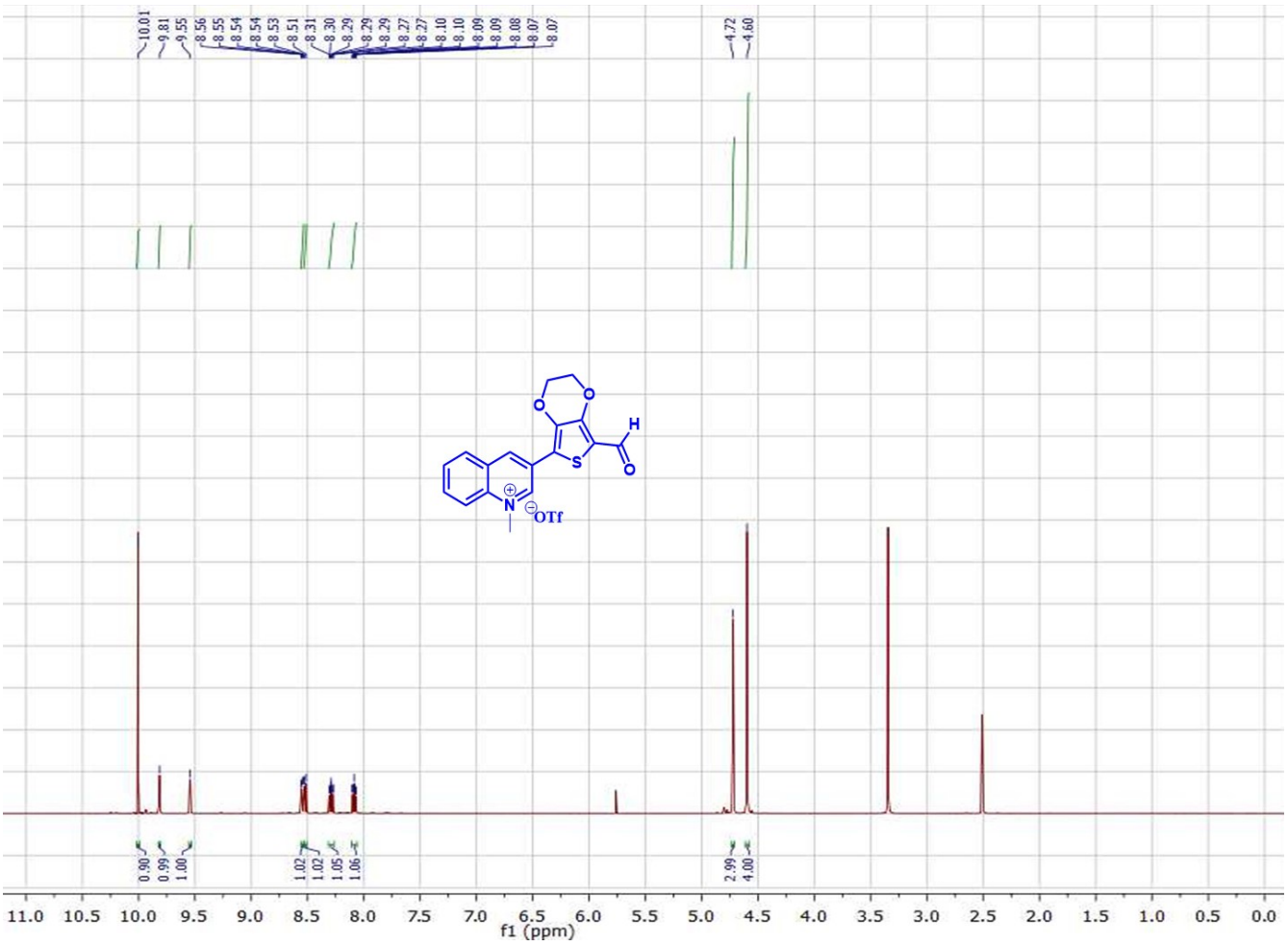

Figure S7: ^{1}H NMR spectrum of Probe **B** in DMSO-d_6 solution.

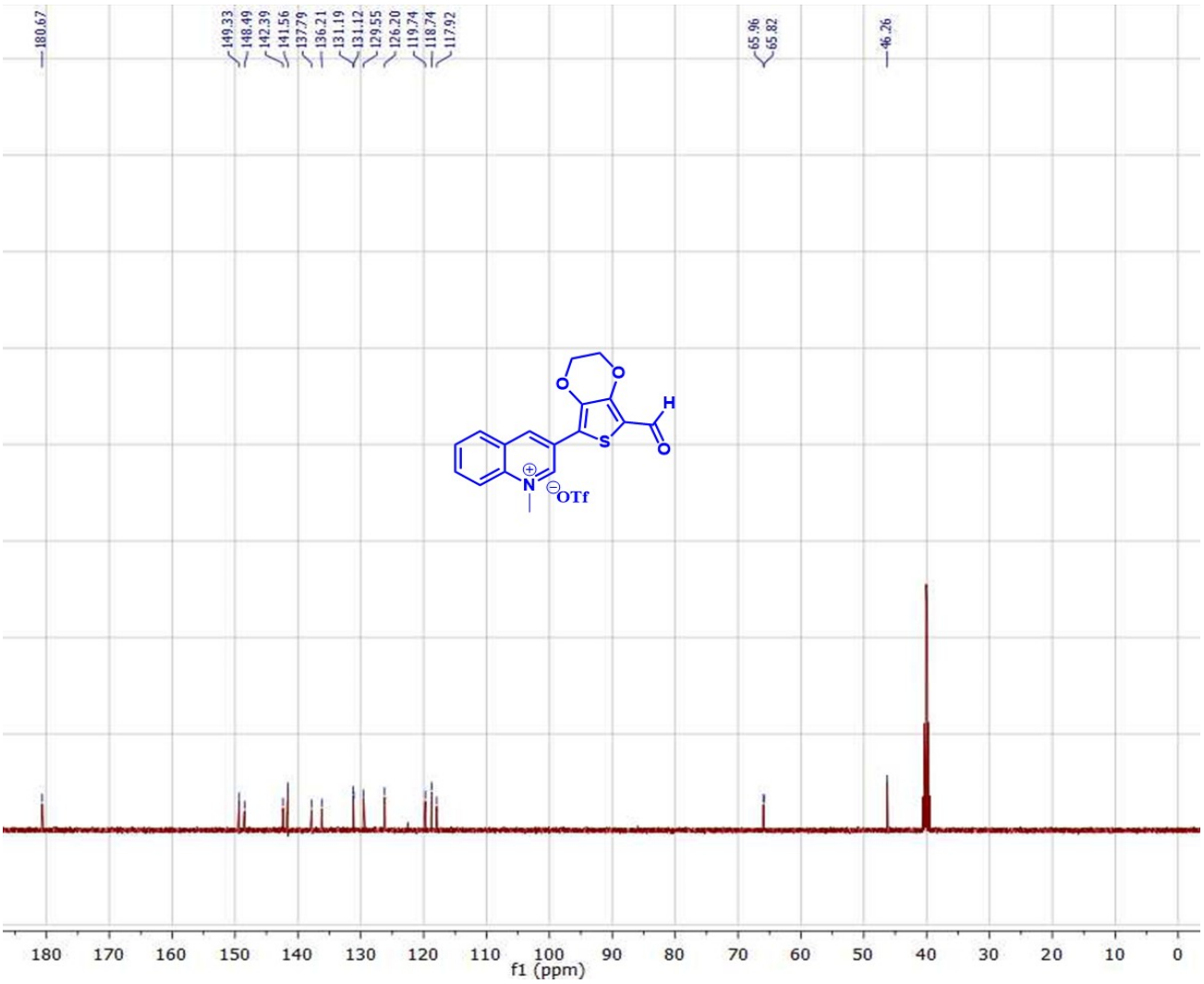

Figure S8: ^{13}C NMR spectrum of Probe **B** in DMSO-d_6 solution.

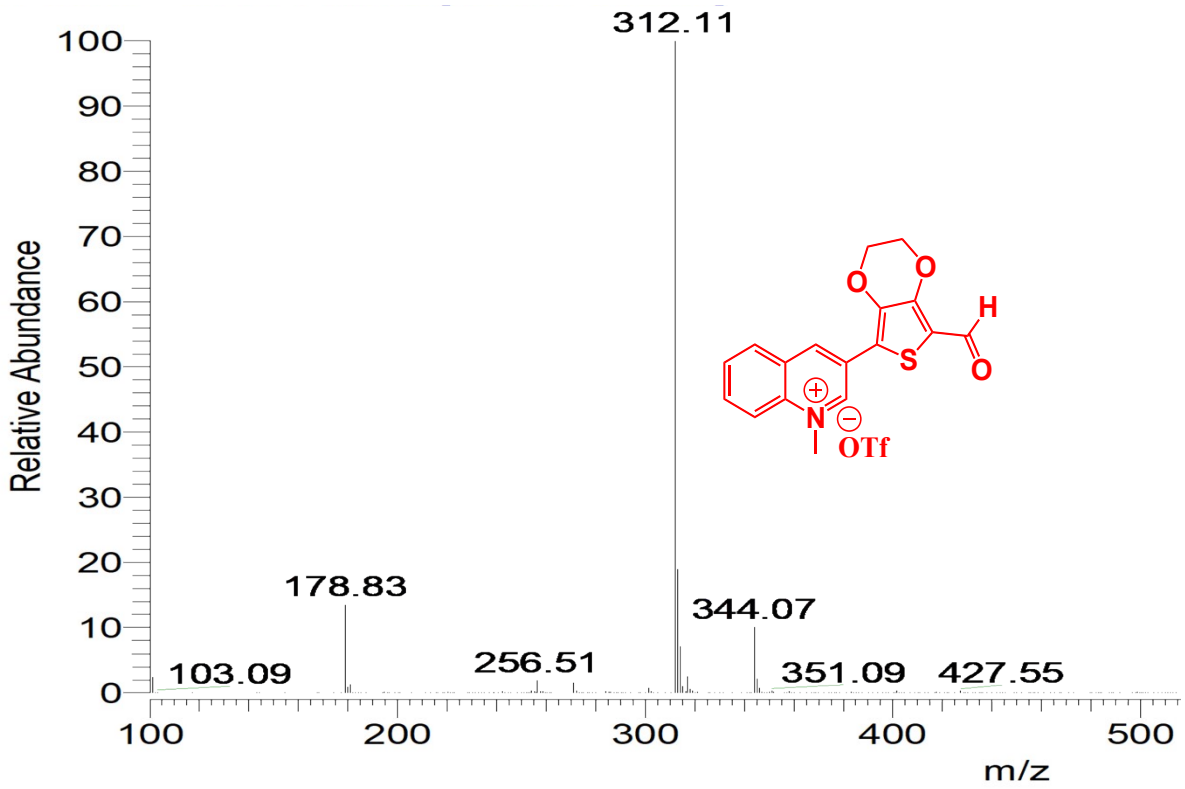

Figure S9: Electrospray MS spectrum of Probe **B**.

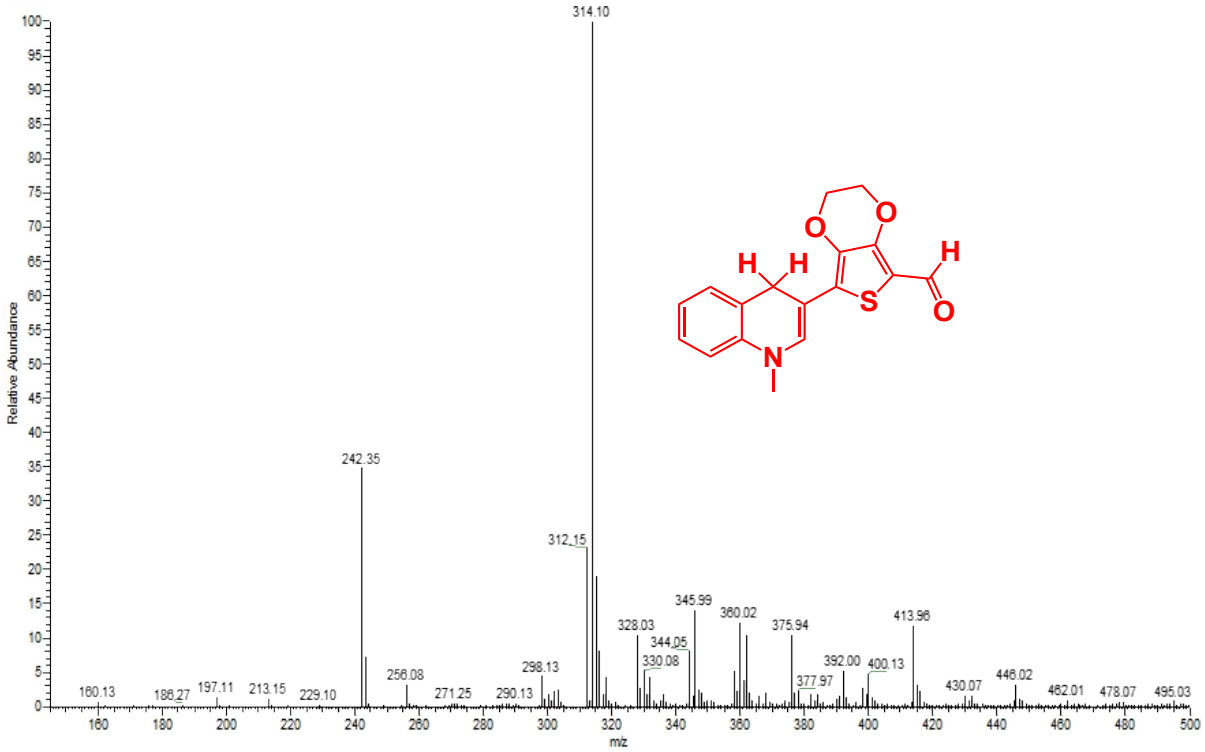

Figure S10: Electrospray MS spectrum of Probe **BH**.

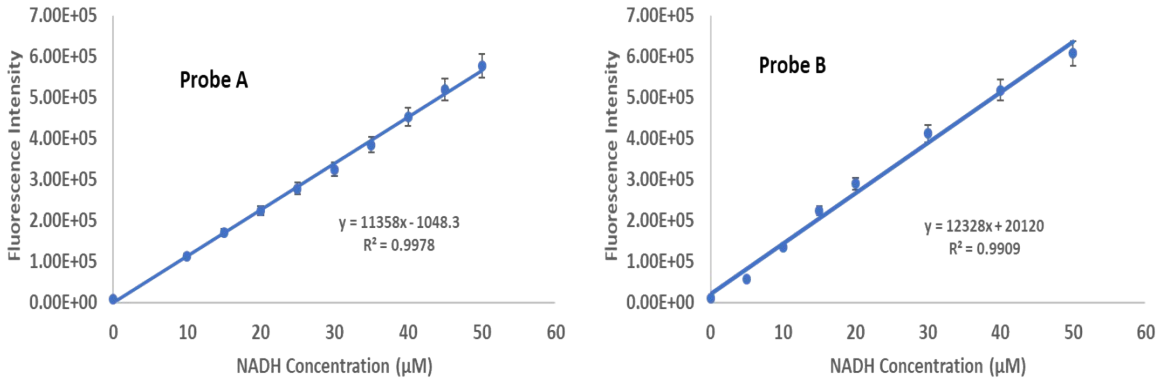

Figure S11. Fluorescence intensity changes of Probe **A** and Probe **B** (5 μM) with different concentration of NADH (0-50 μM) with four repeated measures. Probes **A** and **B** have a detection limit of 0.03 μM and 0.02 μM, respectively.

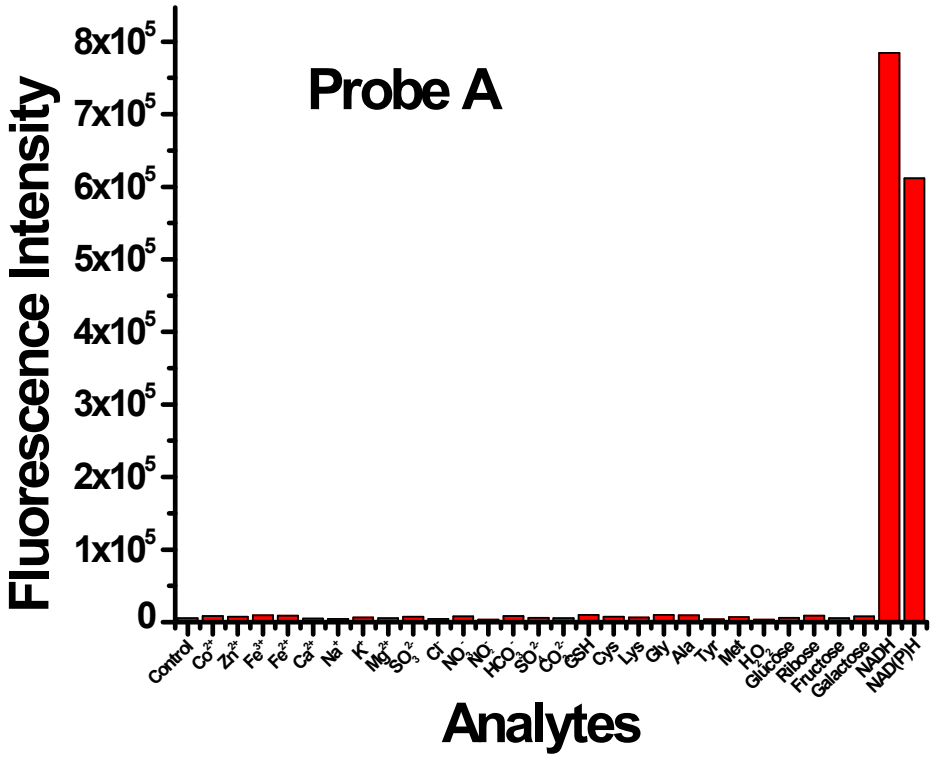

Figure S12. The fluorescence response of Probe **A** at a concentration of 5 μM to various species at 0.1 mM was measured.

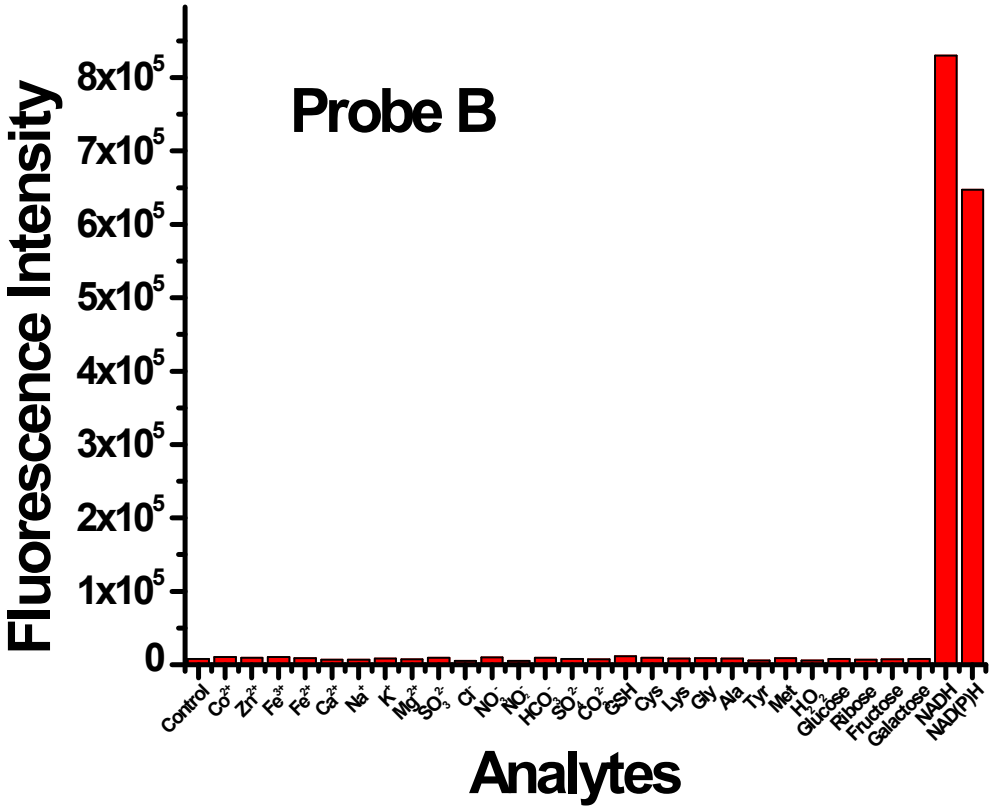

Figure S13. The fluorescence response of Probe **B** at a concentration of 5 μM to various species at 0.1 mM was measured.

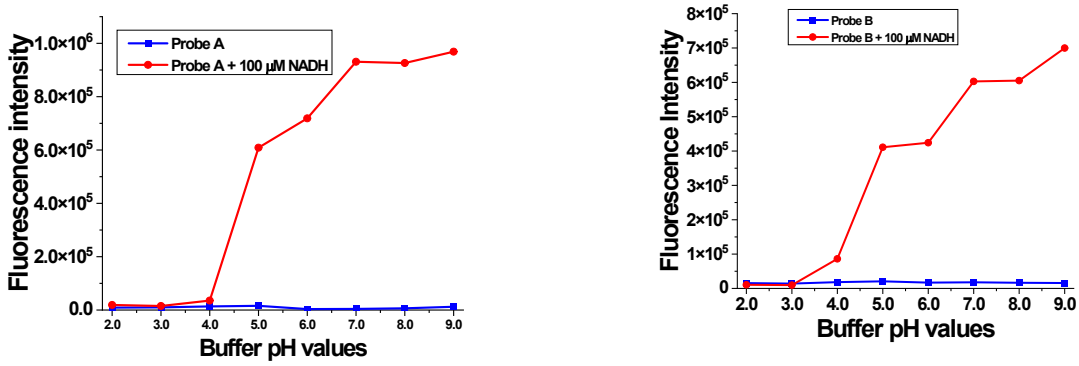

Figure S14. The fluorescence responses of Probes **A** and **B** in the absence and presence of 0.1 M NADH in different pH buffers.

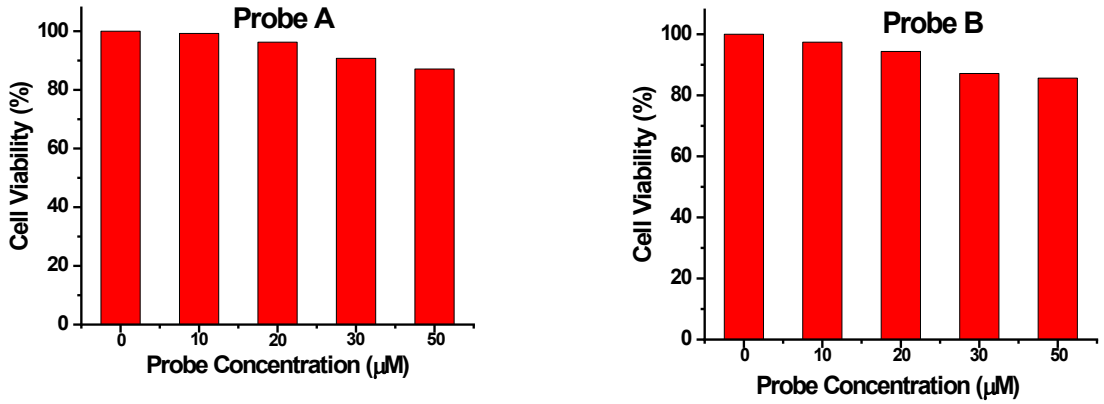

Figure S15. MTT assay of A549 cells incubated with Probes **A** (left) and **B** (right) with different concentrations.

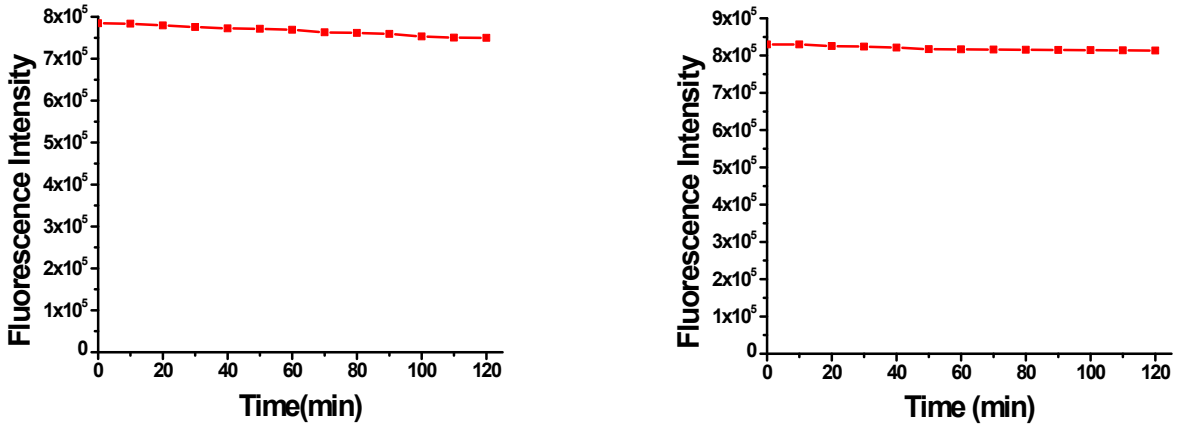

Figure S16. Photostability of 5 μM Probes **A** and **B** in the presence of NADH (100 μM).

To compare the imaging capabilities of our probe **A** with a fluorescent probe reported in ACS Sensors 2016, 6(1), 702-709 (Scheme 2), we synthesized and characterized the latter probe by NMR and MS spectrometers and investigated its fluorescence response to NADH. We first examined the probe's optical responses to varying concentrations of NADH. Our findings showed that the probe's fluorescence intensity increased with increasing NADH concentration from 0 to 10 µM. However, at higher concentrations, the probe exhibited fluorescence quenching (Figure 18), limiting its imaging capabilities as we demonstrated later in Figures (S19 and S20).

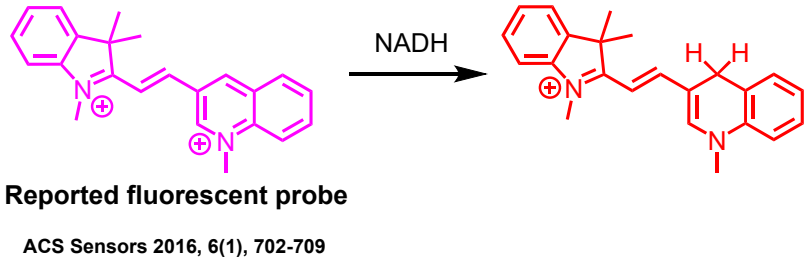

Scheme 2. Chemical structures of a reported fluorescent probe in response to NADH.

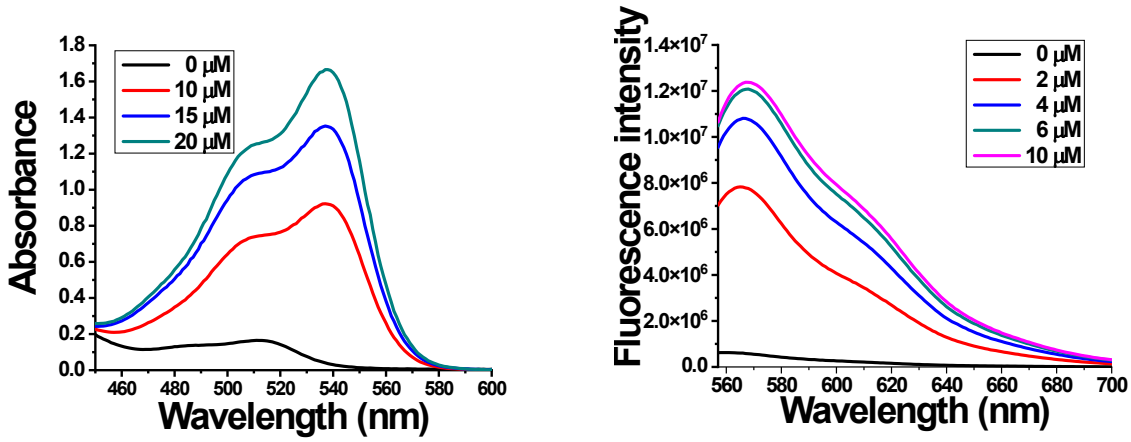

Figure S17. Absorption and fluorescence spectra of 20 µM fluorescent probe (reported in ACS Sensors 2016, 6, 702-709) in pH 7.4 PBS buffer containing 5% DMSO solution in the absence and presence of different NADH concentrations under 537 nm excitation.

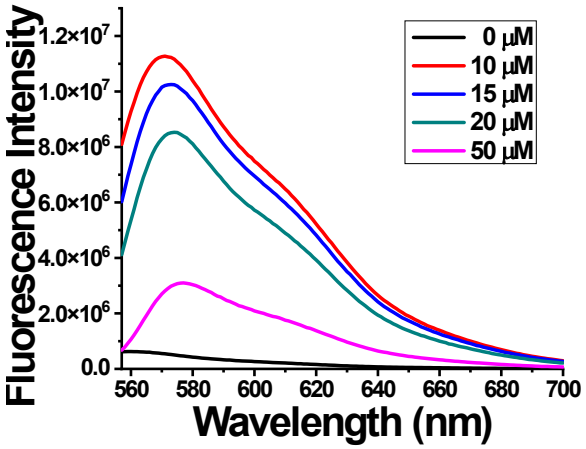

Figure S18. Fluorescence spectra of 20 μM fluorescent probe (reported in ACS Sensors 2016, 6, 702-709) in pH 7.4 PBS buffer containing 5% DMSO solution in the absence and presence of different NADH concentrations under 537 nm excitation.

Gemcitabine is a chemotherapeutic drug classified as an antimetabolite that has been utilized for treating various types of cancer.[1-4] By disrupting the process of DNA replication, gemcitabine has been reported to have antitumor effects.[1-4] Moreover, it has been shown to affect cellular metabolism and energy production.[1-4] Figure S19 shows that various concentrations of gemcitabine increased the levels of NAD(P)H in A459 cancer cells. These coenzymes exert an important role in metabolic pathways such as glycolysis and the citric acid cycle, which are fundamental for cellular respiration and ATP production. The precise mechanisms underlying the ability of gemcitabine to increase NAD(P)H levels are not yet fully elucidated, but it is hypothesized that inhibition of ribonucleotide reductase by gemcitabine may trigger a decline in deoxynucleotide levels, leading to a compensatory rise in NAD(P)H levels. These coenzymes are also essential for other metabolic pathways and energy production. Gemcitabine-induced increases in NAD(P)H levels may result from its antitumor effects by changing cellular metabolism and energy production, resulting in cellular stress and ultimately apoptosis. However, further research is needed to fully understand the mechanisms and clinical implications of gemcitabine-induced changes in NAD(P)H levels in cancer cells.

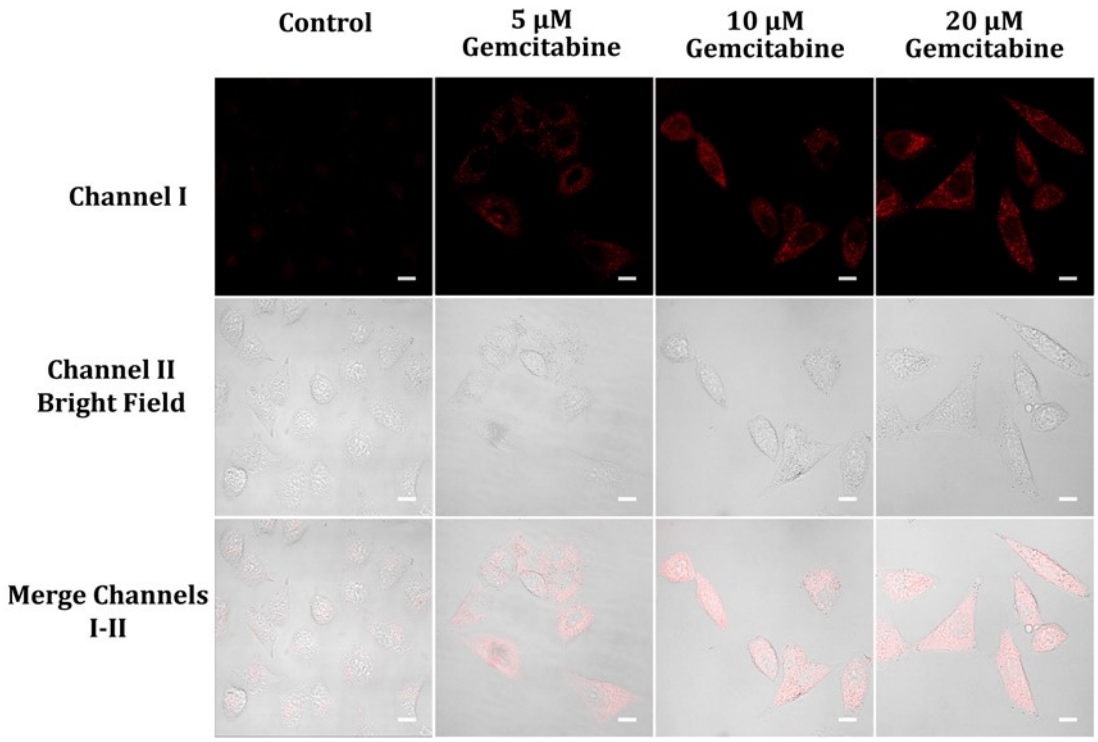

Figure S19. Fluorescence images of A459 cells pre-treated with various concentrations of gemcitabine in glucose-deficient DMEM medium for two hours, followed by incubation with 5 µM Probe **A** in cell medium for 30 minutes. The cellular fluorescence was acquired using a 488 nm excitation and emission was collected within the range of 575-675 nm. The scale bars represent 50 µm.

In our study, we used a fluorescent probe previously reported in ACS Sensors, 2016, 6(1), 702-709 to investigate the effects of gemcitabine treatment on NAD(P)H levels in A459 cells under the same identification conditions for comparison purposes. Treatment of A459 cells with 5 µM of the reported probe resulted in a significant increase in NAD(P)H levels, which was consistent with the results obtained using probe **A**. However, increasing the concentration of gemcitabine beyond 10 µM led to a decrease in cellular fluorescence due to fluorescence quenching resulting from an increase in NADH concentration (as shown in Figure 18). This indicates that the reported probe is not suitable for monitoring significant changes in NAD(P)H levels in live cells. On the other hand, Figure S19 shows that our probe **A** effectively monitored different concentrations of gemcitabine-induced changes in NAD(P)H levels in A459 cancer cells. Therefore, our probe is a

suitable tool for monitoring significant changes in NAD(P)H levels in live cells under different chemical treatments (Figures S19, 7-8, 10-14).

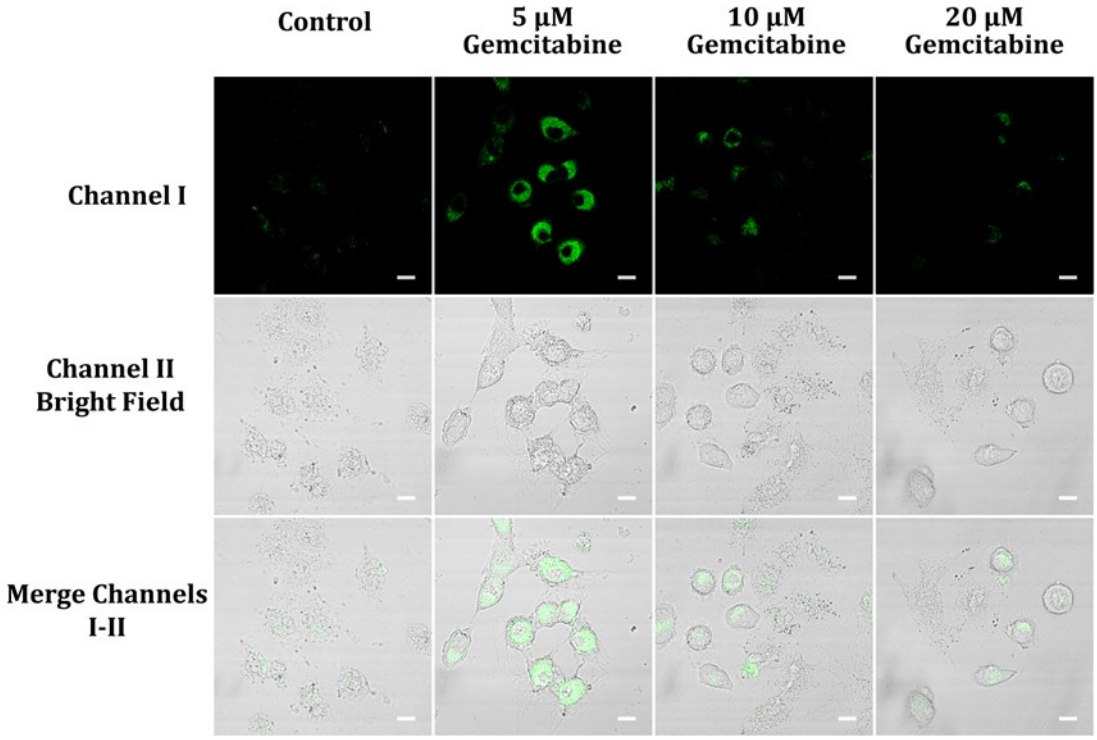

Figure S20. Fluorescence images of A459 cells treated with different concentrations of gemcitabine in glucose-deficient DMEM medium for two hours, followed by incubation with 5 µM of a fluorescent probe (previously reported in ACS Sensors, 2016, 6(1), 702-709) in serum-free DMEM medium for 30 minutes. The cells were excited at 488 nm and the emitted fluorescence was collected between 500-600 nm. The scale bars in the images correspond to 50 µm.

Theoretical Calculations

Methods:

Models of Probes **A**, **AH**, **B**, and **BH** were generated through the use of Gaussian 16 and density functional theory (DFT), using the APFD functional and electron basis sets at the 6-311+g(d,p) for optimization of the geometry in a Polarizable Continuum Model (PCM) of water. Upon confirming the lack of imaginary frequencies, the CAM-B3LYP/6-311+g(d,p) basis set was used in a TD-DFT calculation to calculate the absorption energies. Results were interpreted using GaussView 6 for all data and figures.

Results of Theoretical Calculations:

Theoretical Calculations for probe **A**

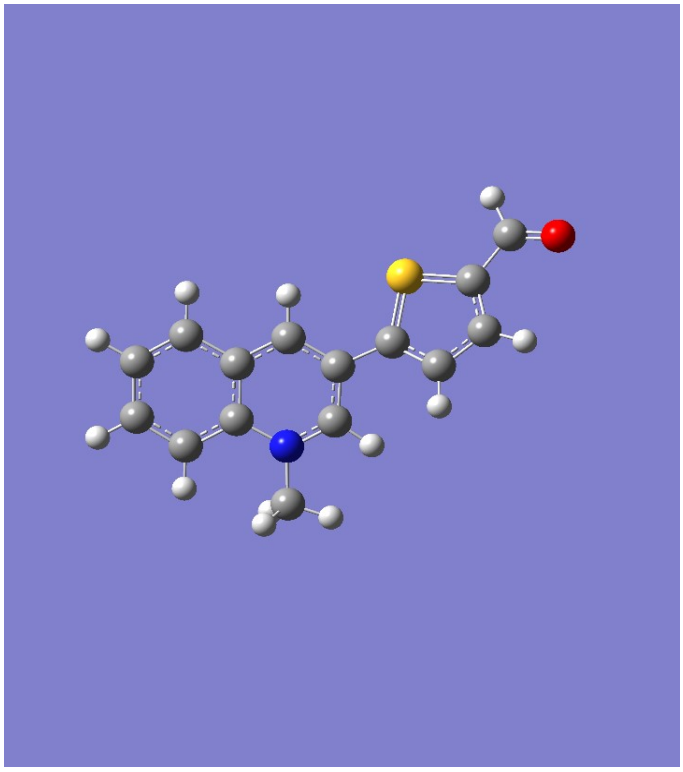

Figure 21: GaussView representation of probe **A** optimized geometry.

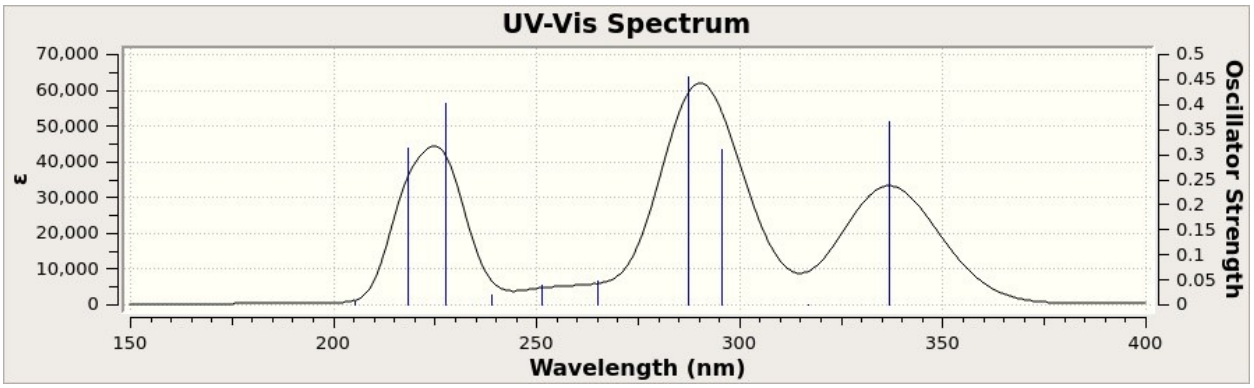

Figure S22: Calculated UV-Vis spectrum for Probe **A** in water.

Table S1: Calculated atomic coordinated for Probe **A** in water.

Row	Symbol	X	Y	Z	Row	Symbol	X	Y	Z
1	C	-4.291870	-2.041579	-0.180606	16	S	2.381733	-1.006958	0.432633
2	C	-4.949180	-0.804393	-0.023352	17	C	5.142304	-0.790921	0.247427
3	C	-4.245050	0.373455	0.085860	18	O	6.194380	-0.243924	-0.020885
4	C	-2.841538	0.337664	0.040098	19	H	5.128411	-1.804309	0.689989
5	C	-2.163050	-0.901686	-0.118163	20	H	-4.874803	-2.952007	-0.264056
6	C	-2.922897	-2.090200	-0.228533	21	H	-6.032877	-0.775900	0.012232

7	N	-2.080337	1.483891	0.149169	22	H	-4.778729	1.306818	0.204807
8	C	-0.754908	1.445934	0.107621	23	H	-2.398968	-3.032056	-0.350079
9	C	-0.035776	0.255041	-0.066496	24	H	-0.249838	2.394509	0.230066
10	C	-0.760833	-0.916711	-0.175413	25	H	-0.254081	-1.865597	-0.321705
11	C	-2.742523	2.782765	0.329890	26	H	-3.322053	2.768196	1.252164
12	C	1.420871	0.308669	-0.124585	27	H	-1.981666	3.555442	0.390372
13	C	2.205307	1.341652	-0.599528	28	H	-3.390712	2.978457	-0.523218
14	C	3.579131	1.063991	-0.519510	29	H	1.798941	2.254141	-1.018390
15	C	3.842003	-0.178048	0.016269	30	H	4.364025	1.733983	-0.847290

Table S2: Excitation energies and oscillator strengths listing for Probe **A** in water.

Excited State	**Nature**	**E (eV)**	**□□(nm)**	***f***	**Orbital transitions**	**Normalized coefficient**
1:	A	3.6801	336.90	0.3662	66 -> 67	0.68032
2:	A	3.9117	316.96	0.0003	63 -> 67	-0.28161
					63 -> 68	0.51882
					63 -> 69	-0.32264
					63 -> 72	0.14713
3:	A	4.1936	295.65	0.3108	62 -> 67	-0.16517
					64 -> 67	-0.11120
					64 -> 69	0.10283
					65 -> 67	-0.18911
					66 -> 68	0.61875
Excited State	**Nature**	**E (eV)**	**□□(nm)**	***f***	**Orbital transitions**	**Normalized coefficient**
4:	A	4.3160	287.26	0.4548	62 -> 68	0.11158
					64 -> 67	0.35188
					65 -> 67	0.51361
					66 -> 68	0.25524
					66 -> 69	-0.13535
5:	A	4.6805	264.89	0.0488	64 -> 67	0.50796
					64 -> 68	-0.24024
					65 -> 67	-0.31545
					65 -> 68	0.21527
6:	A	4.9311	251.43	0.0398	62 -> 67	0.53322
					62 -> 68	0.13518
					65 -> 67	-0.16183
					65 -> 68	-0.24275
					65 -> 69	-0.10774
					66 -> 67	0.13206
					66 -> 68	0.13209
					66 -> 69	-0.16770
7:	A	5.1892	238.93	0.0183	62 -> 67	-0.11927
					64 -> 67	0.28063

					64 -> 68	0.47569
					65 -> 67	-0.19425
					65 -> 68	-0.31907
8:	A	5.4496	227.51	0.4016	62 -> 67	0.24729
					62 -> 68	-0.10388
					64 -> 68	0.17828
					65 -> 67	0.10716
					66 -> 69	0.58600
9:	A	5.6788	218.33	0.3121	62 -> 67	0.25848
					64 -> 68	0.28912
					64 -> 69	0.13382
					65 -> 68	0.44213
					65 -> 69	0.24417
					66 -> 69	-0.15218
					66 -> 70	-0.11215
10:	A	6.0378	205.35	0.0043	63 -> 67	0.63224
					63 -> 68	0.21384
					63 -> 69	-0.12582
					63 -> 72	0.11099

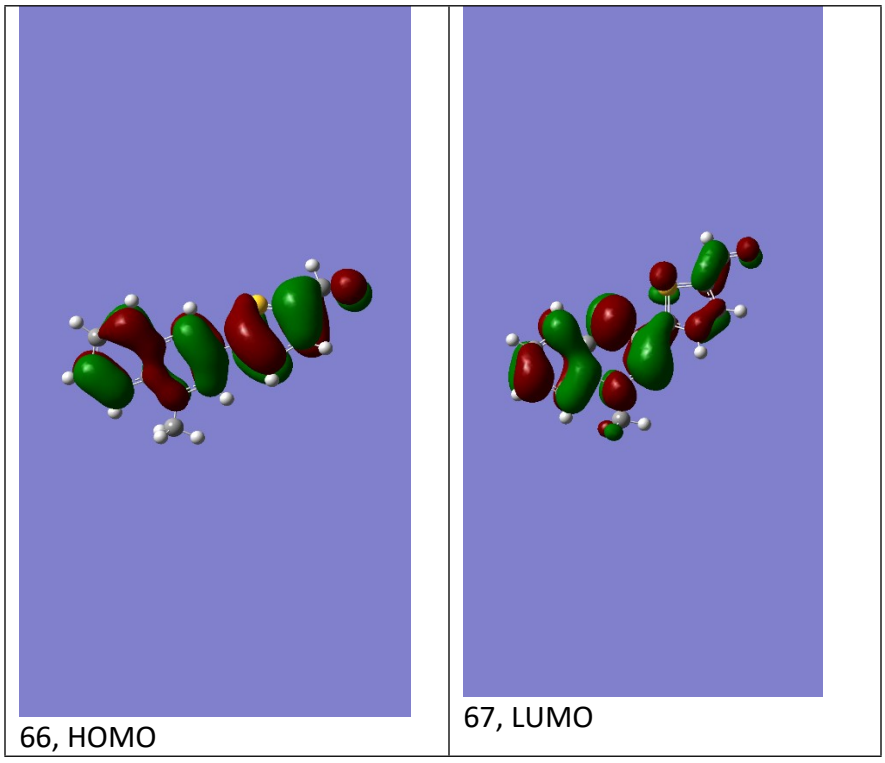

Figure S23: Drawing of selected molecular orbitals listed in Table S1.

Theoretical calculations for Probe **AH**

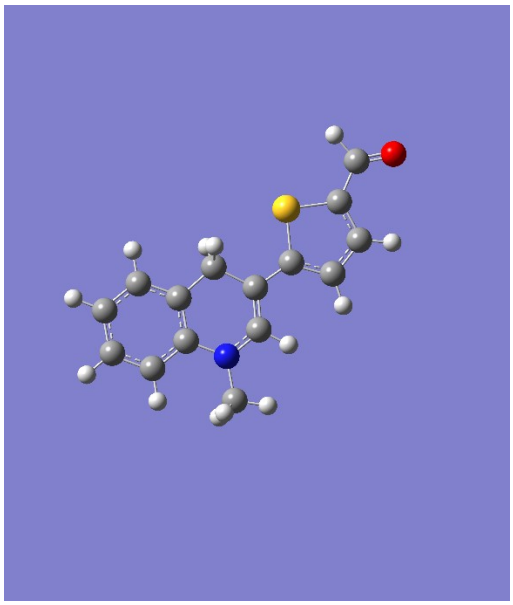

Figure S24: GaussView representation of Probe **AH** optimized geometry.

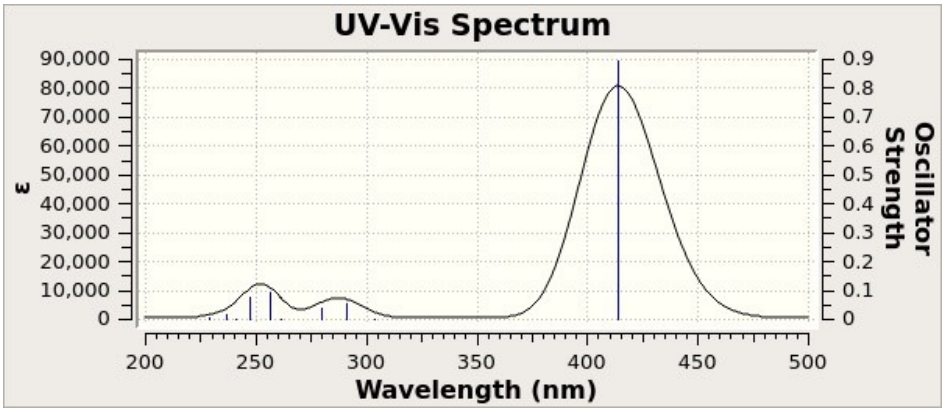

Figure S25: Calculated UV-Vis spectrum for Probe **AH** in water.

Table S3: Calculated atomic coordinated for Probe **AH** in water.

Row	Symbol	X	Y	Z	Row	Symbol	X	Y	Z
1	C	-4.323192	-2.050473	0.060521	17	O	5.126039	-0.872498	-0.005429
2	C	-4.976991	-0.822960	0.059456	18	H	6.221493	-0.321634	0.035697
3	C	-4.247452	0.359419	0.024746	19	H	5.064876	-1.977125	-0.057953
4	C	-2.847261	0.328742	-0.011771	20	H	-4.887107	-2.977083	0.089144
5	C	-2.178331	-0.907749	-0.015196	21	H	-6.061151	-0.777316	0.087275
6	C	-2.932231	-2.076203	0.024190	22	H	-4.776667	1.304269	0.028389
7	N	-2.106735	1.516446	-0.039067	23	H	-2.409478	-3.029294	0.023363
8	C	-0.748144	1.478557	-0.022758	24	H	-0.279227	2.454338	-0.011686
9	C	-0.002641	0.342869	-0.021496	25	H	-0.375765	-1.538525	-0.983962

10	C	-0.674474	-1.002176	-0.069848	26	H	-0.321053	-1.630658	0.760920
11	C	-2.783548	2.800319	-0.045200	27	H	-2.036266	3.590688	-0.077799
12	C	1.430202	0.412370	0.005480	28	H	-3.427574	2.896681	-0.923411
13	C	2.282091	1.519506	0.075161	29	H	-3.387649	2.930153	0.857241
14	C	3.633221	1.183214	0.075012	30	H	1.924477	2.540107	0.128905
15	C	3.867921	-0.182244	0.008753	31	H	4.441752	1.903066	0.125412
16	S	2.359673	-1.049718	-0.056729					

Table S4: Excitation energies and oscillator strengths listed for Probe **AH.**

Excited State	**Nature**	**E (eV)**	**□□(nm)**	***f***	**Orbital transitions**	**Normalized coefficient**
1:	A	2.9934	414.20	0.8941	67 -> 68	0.67970
					67 -> 69	0.13983
.						
2:	A	4.0800	303.88	0.0002	63 -> 68	0.61769
					63 -> 69	-0.28480
3:	A	4.2574	291.22	0.0563	66 -> 68	-0.19527
					67 -> 68	-0.11712
					67 -> 69	0.63597
4:	A	4.4270	280.06	0.0378	65 -> 68	-0.10648
					66 -> 70	-0.17557
					67 -> 70	0.64299
5:	A	4.7439	261.35	0.0009	67 -> 71	0.64193
					67 -> 75	0.14325
					67 -> 77	-0.13143
					67 -> 78	0.10390
6:	A	4.8388	256.23	0.0904	62 -> 68	-0.13203
					64 -> 68	0.18129
					66 -> 68	0.61720
					66 -> 69	0.10296
					67 -> 69	0.17047
7:	A	5.0143	247.26	0.0736	64 -> 68	0.61618
					65 -> 68	0.19437
					66 -> 68	-0.16313
					67 -> 69	-0.12373
8:	A	5.1487	240.81	0.0002	67 -> 72	-0.29191
					67 -> 75	0.38124
					67 -> 76	-0.22231
					67 -> 77	-0.24234
					67 -> 78	-0.16399
					67 -> 83	0.20902
					67 -> 85	0.11189

9:	A	5.2367	236.76	0.0164	64 -> 68 66 -> 69 67 -> 74	-0.11951 0.15377 0.64127
Excited State	**Nature**	**E (eV)**	**□□(nm)**	***f***	**Orbital transitions**	**Normalized coefficient**
10:	A	5.4214	228.69	0.0071	66 -> 71 67 -> 72 67 -> 73 67 -> 75 67 -> 76 67 -> 79 67 -> 82	0.13028 0.53869 -0.10691 0.23979 -0.19154 -0.14756 -0.17360

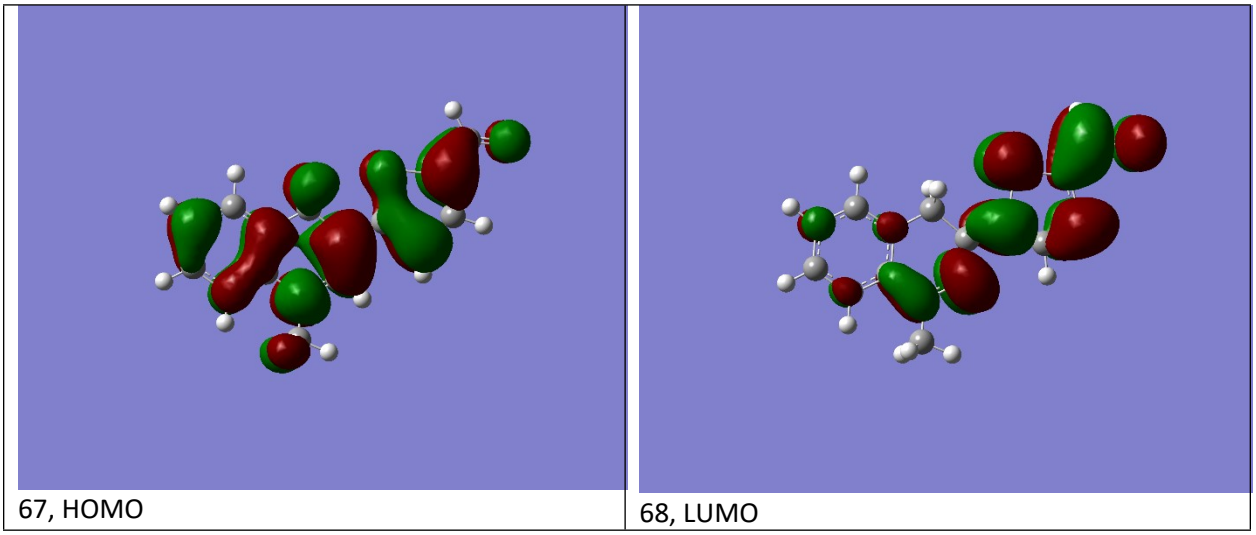

67, HOMO | 68, LUMO

Figure S26: Drawings of selected molecular orbitals listed in Table S2.

Theoretical calculations for probe **B.**

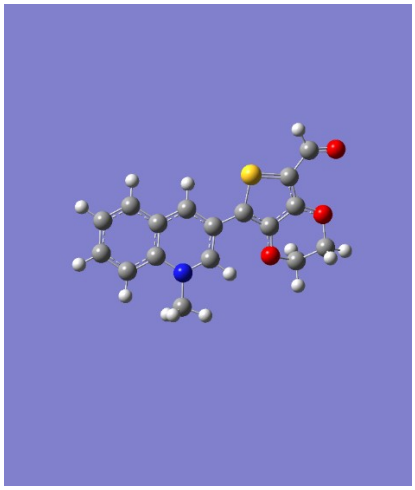

Figure S27: GaussView representation of Probe **B** optimized geometry.

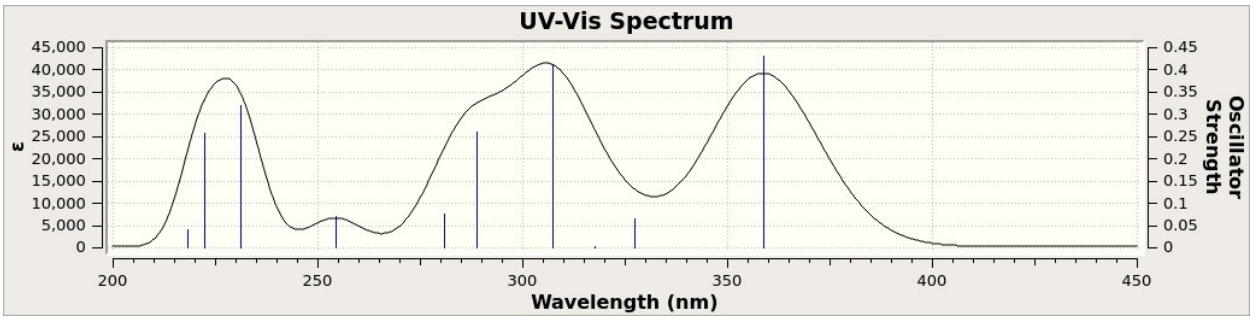

Figure S28: Calculated UV-Vis spectrum for Probe **B.**

Table S5: Calculated atomic coordinated for Probe **B** in water.

Row	Symbol	X	Y	Z	Row	Symbol	X	Y	Z
1	C	5.235363	-1.717320	-0.406222	19	H	-3.926040	-3.259370	0.406748
2	C	5.699053	-0.411222	-0.146401	20	O	-1.495234	1.924993	-0.259665
3	C	4.825319	0.623416	0.100053	21	C	-2.634831	2.626921	-0.785448
4	C	3.443904	0.368693	0.092866	22	C	-3.887874	2.239684	-0.033047
5	C	2.959458	-0.941955	-0.166771	23	O	-4.157609	0.832451	-0.170412
6	C	3.890032	-1.978906	-0.417233	24	H	5.948386	-2.511577	-0.597206
7	N	2.518317	1.362732	0.333591	25	H	6.765594	-0.213982	-0.140129
8	C	1.213613	1.122194	0.330145	26	H	5.210424	1.615175	0.295488
9	C	0.678631	-0.151158	0.070123	27	H	3.514473	-2.977101	-0.615067
10	C	1.576655	-1.174714	-0.179326	28	H	0.573412	1.967145	0.538180
11	C	2.975603	2.731433	0.607190	29	H	1.223180	-2.177641	-0.398347
12	C	-0.761030	-0.347273	0.079749	30	H	3.531488	3.105231	-0.252069
13	C	-1.743032	0.611035	-0.076417	31	H	2.106093	3.359307	0.777475
14	C	-3.061309	0.074803	-0.043542	32	H	3.605127	2.733088	1.496139
15	C	-3.069471	-1.298888	0.123571	33	H	-2.421773	3.687610	-0.662130
16	S	-1.453079	-1.917090	0.269619	34	H	-2.728271	2.393540	-1.850524
17	C	-4.193739	-2.200452	0.223454	35	H	-4.757690	2.753766	-0.439414
18	O	-5.360997	-1.866256	0.120506	36	H	-3.790703	2.471864	1.031906

Table S6: Excitation energies and oscillator strengths for Probe **B** in water.

Excited State	Nature	E (eV)	□□(nm)	*f*	Orbital transitions	Normalized coefficient
1:	A	3.4543	358.92	0.4319	81 -> 82	0.68702
2:	A	3.7877	327.34	0.0647	80 -> 82	0.64207
					80 -> 83	0.23089
3:	A	3.9046	317.53	0.0020	78 -> 82	0.33041
					78 -> 83	0.47862
					78 -> 84	0.31927
					78 -> 90	0.13540
4:	A	4.0326	307.45	0.4110	77 -> 82	0.12792
					79 -> 84	-0.10974
					80 -> 83	-0.12732
					81 -> 83	0.65408
5:	A	4.2933	288.79	0.2597	77 -> 83	-0.10558
					79 -> 82	0.64670
					80 -> 83	-0.11337
					81 -> 83	-0.13378
					81 -> 84	-0.12592
6:	A	4.4134	280.92	0.0759	77 -> 82	0.15253
					80 -> 82	-0.23737
					80 -> 83	0.61318
					80 -> 84	0.10564
7:	A	4.8744	254.36	0.0716	77 -> 82	0.53749
					77 -> 83	-0.12904
					79 -> 82	-0.11811
					79 -> 83	0.24012
					79 -> 84	-0.13238
					80 -> 83	-0.11294
					81 -> 82	0.11098
					81 -> 83	-0.13113
					81 -> 84	-0.16112
8:	A	5.3651	231.10	0.3200	77 -> 82	0.24265
					81 -> 84	0.60172

Excited State	Nature	E (eV)	□□(nm)	*f*	Orbital transitions	Normalized coefficient
9:	A	5.5760	222.36	0.2567	77 -> 82	0.18884
					79 -> 83	-0.35199
					79 -> 84	0.15573

					80 -> 84	0.44437
					80 -> 89	-0.12092
					81 -> 84	-0.14152
10:	A	5.6812	218.24	0.0403	79 -> 83	-0.20490
					80 -> 85	0.12475
					80 -> 87	-0.31893
					80 -> 88	-0.26514
					80 -> 89	0.32027
					80 -> 93	-0.10019
					80 -> 94	0.12582
					80 -> 97	0.15705
					80 -> 98	0.12716

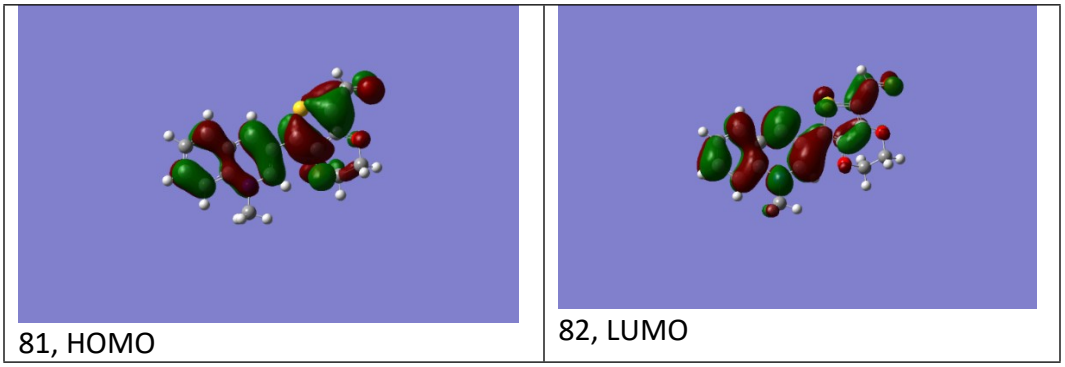

Figure S29: Drawings of selected molecular orbitals listed in Table S3.

Theoretical calculations for Probe **BH.**

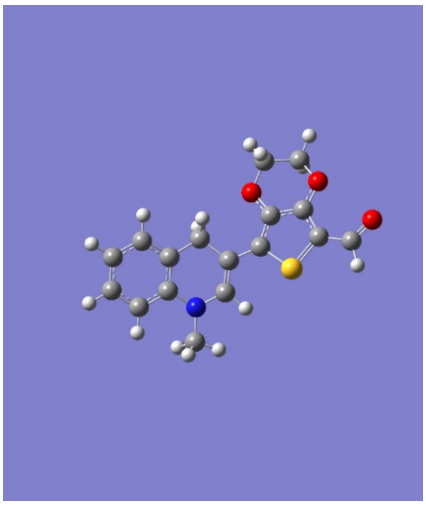

Figure S30: GaussView representation of Probe **BH** optimized geometry.

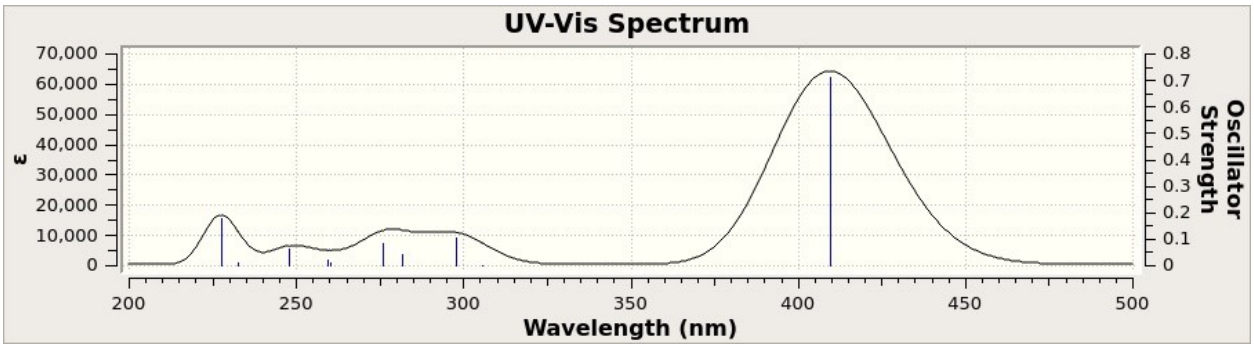

Figure S31: Calculated UV-Vis spectrum for Probe **BH** in water.

Table S7: Calculated atomic coordinated of Probe **BH** in water.

Row	Symbol	X	Y	Z	Row	Symbol	X	Y	Z
1	C	4.360901	1.600966	-0.787839	20	O	-2.000181	1.770751	0.626221
2	C	4.955463	0.363083	-0.569504	21	C	-3.001704	2.768861	0.411534
3	C	4.184862	-0.728933	-0.183966	22	C	-4.371921	2.228717	0.760970
4	C	2.804205	-0.588560	0.002404	23	O	-4.713863	1.108834	-0.072993
5	C	2.198345	0.666522	-0.190107	24	H	4.957183	2.453481	-1.096550
6	C	2.987126	1.735823	-0.599293	25	H	6.024792	0.235599	-0.707026
7	N	2.005032	-1.683970	0.347178	26	H	4.665158	-1.688982	-0.038467
8	C	0.647787	-1.594545	0.208771	27	H	2.511999	2.700770	-0.756596
9	C	-0.023970	-0.432354	0.019361	28	H	0.125759	-2.543705	0.266693
10	C	0.732020	0.871337	0.097330	29	H	0.315801	1.599678	-0.604013
11	C	2.606151	-2.981888	0.586327	30	H	0.609684	1.320263	1.093367
12	C	-1.444678	-0.431819	-0.211295	31	H	1.827859	-3.676964	0.896130
13	C	-2.346677	0.589154	0.047762	32	H	3.089379	-3.374526	-0.314876
14	C	-3.686453	0.269421	-0.283223	33	H	3.346131	-2.919123	1.387528
15	C	-3.826486	-1.004143	-0.821628	34	H	-2.745667	3.609123	1.056342
16	S	-2.265721	-1.782302	-0.923440	35	H	-2.969210	3.092054	-0.635358
17	C	-5.002202	-1.698485	-1.248134	36	H	-5.143550	2.978783	0.590347
18	O	-6.139365	-1.238980	-1.265375	37	H	-4.403409	1.905568	1.806396
19	H	-4.822552	-2.739737	-1.585030					

Table S8: Excitation energies and oscillator strengths listing for Probe **BH** in water.

Excited State	Nature	E (eV)	□□(nm)	*f*	Orbital transitions	Normalized coefficient
1:	A	3.0272	409.57	0.7114	82 -> 83	0.68254
2:	A	4.0569	305.61	0.0023	77 -> 83	0.11931
					78 -> 83	0.61383
					78 -> 84	-0.16308
					78 -> 85	0.13734
					78 -> 86	-0.11236
3:	A	4.1616	297.92	0.1069	80 -> 83	0.12686
					81 -> 83	0.67495
4:	A	4.4037	281.54	0.0418	80 -> 83	-0.31685
					80 -> 84	-0.10837
					82 -> 84	0.57921
5:	A	4.4925	275.98	0.0858	77 -> 83	0.10110
					80 -> 83	-0.35180
					80 -> 84	0.11357
					82 -> 84	-0.13232
					82 -> 85	-0.37100
					82 -> 86	0.38313
6:	A	4.7604	260.45	0.0104	80 -> 83	-0.12620
					82 -> 85	0.46880
					82 -> 86	0.30841
					82 -> 87	-0.16211
					82 -> 89	-0.23775
					82 -> 90	0.13351
					82 -> 92	-0.13497
7:	A	4.7782	259.48	0.0206	77 -> 83	-0.12863
					80 -> 83	0.40893
					81 -> 83	-0.13548
					82 -> 83	-0.10664
					82 -> 84	0.25993
					82 -> 86	0.39611

Excited State	Nature	E (eV)	□□(nm)	*f*	Orbital transitions	Normalized coefficient
8:	A	4.9991	248.01	0.0622	80 -> 83	-0.13503

					82 -> 85	0.20814
					82 -> 87	0.31692
					82 -> 88	-0.14443
					82 -> 89	0.34405
					82 -> 90	0.20212
					82 -> 92	0.10601
					82 -> 93	0.16698
					82 -> 98	0.10404
9:	A	5.3320	232.53	0.0089	80 -> 85	0.12021
					82 -> 87	0.44714
					82 -> 88	0.32791
					82 -> 89	-0.15223
					82 -> 92	-0.18329
					82 -> 96	0.22105
10:	A	5.4502	227.49	0.1756	79 -> 83	0.17963
					80 -> 84	0.14928
					80 -> 85	-0.10154
					82 -> 84	0.13795
					82 -> 90	0.47696
					82 -> 91	-0.26730

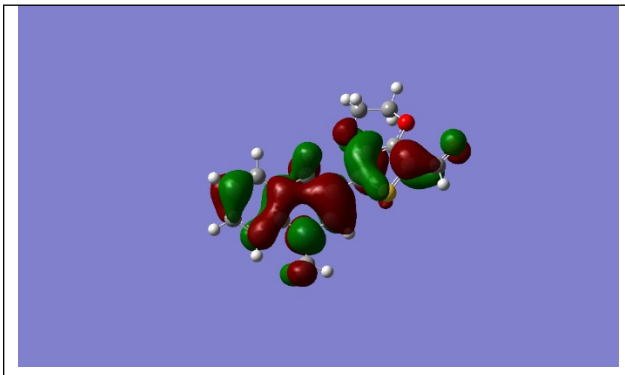

82, HOMO

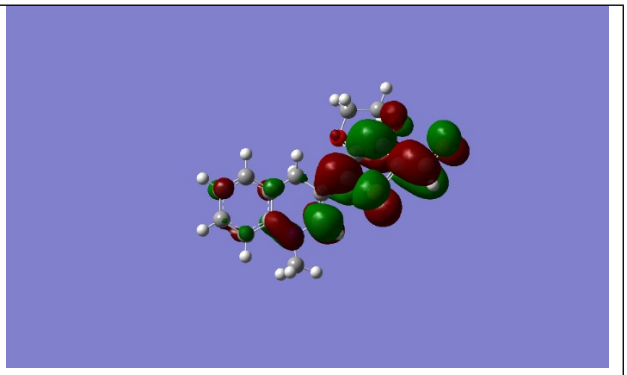

83, LUMO

Figure S32: Drawings of selected molecular orbitals listed in Table S4.

References

1. B. H. Dingle, R. B. Rumble, M. C. Brouwers and E. Canc Care Ontarios Program, *Can. J. Gastroenterol. Hepatol.*, 2005, **19**, 711-716.
2. S. Dent, H. Messersmith and M. Trudeau, *Breast Cancer Res. Treat.*, 2008, **108**, 319-331.
3. N. Silvestris, S. Cinieri, I. La Torre, G. Pezzella, G. Numico, L. Orlando and V. Lorusso, *Breast*, 2008, **17**, 220-226.
4. M. D. Shelley, G. Jones, A. Cleves, T. J. Wilt, M. D. Mason and H. G. Kynaston, *BJU Int.*, 2012, **109**, 496-505.